

that spiroannulation results in lengthening of distal bonds ($\alpha = 0.018 \text{ \AA}$), and shortening of bonds vicinal to spiro atoms ($\beta = 0.032 \text{ \AA}$). The corresponding average values for terminal three-membered rings in compounds (3)–(8) are $\alpha = 0.020$ and $\beta = 0.028 \text{ \AA}$. Disubstituted cyclopropanes in (5)–(8) exhibit further shortening of the bonds connecting two spiro atoms. However, the corresponding β' value differs slightly from the additive one ($\beta' = 2\beta - 0.012 = 0.046 \text{ \AA}$). We have found that these three parameters, namely α , β and β' , and the standard value of C—C bond length in cyclopropane ($C = 1.508 \text{ \AA}$; Allen, 1980) can be used for correctly predicting bond lengths for all types of C—C bonds in triangulanes (3)–(8). Estimated values (Tables 5 and 6) for different types of C—C bonds in the triangulanes (for definitions see Fig. 3) are: $D = C + \alpha = 1.528$, $E = C - \beta' = 1.463$, $L = C + \alpha - 2\beta = 1.481$, $M = C - \beta = 1.480$, $N = C + \alpha - \beta = 1.500 \text{ \AA}$.

In conclusion, the X-ray structural study of triangulanes (7) and (8) allowed us to calculate an empirical scheme, providing an accurate description of the geometries of triangulanes (3)–(8), and hopefully, of other possible triangulanes.

References

- ALLEN, F. H. (1980). *Acta Cryst.* **B36**, 81–96.
 BOEZE, R., BASER, D., GOMANN, K. & BLINKER, U. H. (1989). *J. Am. Chem. Soc.* **111**, 1501–1503.
 BOEZE, R., MIEBACH, T. & DEMEIJERE, A. (1991). *J. Am. Chem. Soc.* **113**, 1743–1748.
 IOFFE, A. I., SVYATKIN, V. A. & NEFEDOV, O. M. (1987). *Izv. Akad. Nauk SSSR Ser. Khim.* **4**, 801–807.
 KOZHUSHKOV, S. I., YUFIT, D. S., LUKIN, K. A., BOEZE, R., DEMEIJERE, A., STRUCHKOV, YU. T. & ZEFIROV, N. S. (1991). *Dokl. Akad. Nauk SSSR*, **320**, 104–107.
 LUKIN, K. A., ANDRIEVSKI, A. A., KOZHUSHKOV, S. I., UGRAK, B. I. & ZEFIROV, N. S. (1991). *J. Org. Chem.* **56**, 6176–6181.
 LUKIN, K. A., MASUNOVA, A. YU., UGRAK, B. I. & ZEFIROV, N. S. (1991). *Tetrahedron*, **47**, 5769–5780.
 RASMUSSEN, K. & TORI, C. (1985). *J. Mol. Struct. Theochem.* **121**, 233–246.
 SHELDRIK, G. M. (1976). *SHELX*. Program for crystal structure determination. Univ. of Cambridge, England.
 SHELDRIK, G. M. (1990). *SHELXTL-Plus*. PC version 4.1. Siemens Analytical X-ray Instruments Inc., Madison, Wisconsin, USA.
 YUFIT, D. S., KOZHUSHKOV, S. I., LUKIN, K. A., DEMEIJERE, A., STRUCHKOV, YU. T. & ZEFIROV, N. S. (1991). *Dokl. Akad. Nauk SSSR*, **323**, 357–362.
 ZEFIROV, N. S., KOZHUSHKOV, S. I., KUZNETZOVA, T. S., KOKOREVA, O. V., UGRAK, B. I., LUKIN, K. A. & TRATCH, S. S. (1990). *J. Am. Chem. Soc.* **112**, 7702–7707.

Acta Cryst. (1993). **B49**, 708–718

'Jumping Crystals': X-ray Structures of the Three Crystalline Phases of (\pm)-3,4-Di-*O*-acetyl-1,2,5,6-tetra-*O*-benzyl-*myo*-inositol

BY THOMAS STEINER, WINFRIED HINRICHS AND WOLFRAM SAENGER*

Institut für Kristallographie, Freie Universität Berlin, Takustrasse 6, W-1000 Berlin 33, Germany

AND ROY GIGG

Laboratory for Lipid and General Chemistry, National Institute for Medical Research, Mill Hill, London NW7 1AA, England

(Received 17 September 1992; accepted 20 January 1993)

Abstract

(\pm)-3,4-Di-*O*-acetyl-1,2,5,6-tetra-*O*-benzyl-*myo*-inositol, $C_{38}H_{40}O_8$, $M_r = 624.7$ ('jumping crystal'). Three monoclinic crystal forms. Form I, $T = 18^\circ\text{C}$, $P2_1/n$, $a = 28.883$ (3), $b = 15.189$ (2), $c = 15.566$ (2) \AA , $\beta = 100.37$ (1)°, $V = 6717$ (1) \AA^3 , $Z = 8$, $R = 0.090$ for 5788 reflections [$F > \sigma(F)$]. Form II, $T = 18^\circ\text{C}$ [$T = 60^\circ\text{C}$], $P2_1/c$, $a = 14.269$ (2) [14.464 (6)], $b = 14.862$ (2) [14.923 (5)], $c = 16.506$ (3) \AA [16.385 (6) \AA], $\beta = 103.21$ (1)° [102.73 (3)°], $V = 3407$ (1) \AA^3 [3450 (2) \AA^3], $Z = 4$, $R = 0.086$ [0.093] for 3505 [2338] reflections [$F >$

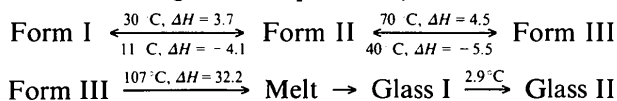
$\sigma(F)$]. Form III, $T = 80^\circ\text{C}$, $P2_1/c$, $a = 16.261$ (8), $b = 15.230$ (8), $c = 14.385$ (7) \AA , $\beta = 96.73$ (4)°, $V = 3533$ (3) \AA^3 , $Z = 4$, $R = 0.083$ for 1651 reflections [$F > \sigma(F)$]. Cu $K\alpha$, Ni-filtered, $\lambda = 1.542 \text{ \AA}$. Phase transitions I \rightarrow II at 30°C , II \rightarrow III at 70°C , III \rightarrow II at 40°C , II \rightarrow I at 11°C . The transitions II \leftrightarrow III are accompanied by vigorous mechanical movements ('thermosalient behaviour') associated with large changes of the unit-cell constants ($\sim 12\%$ change in a and c , and 2.0% in V). The temperature dependence of the unit-cell constants was determined for forms II and III. The principal features of the packing are similar in all crystal forms, but the conformations of the flexible benzyl groups differ to some

* To whom correspondence should be addressed.

extent. They show considerable mobility, as indicated by high temperature factors (and apparent disorder in form I). The reason for the 'jumping' effect is not obvious from the crystal structures.

Introduction

(±)-3,4-Di-*O*-acetyl-1,2,5,6-tetra-*O*-benzyl-*myo*-inositol, C₃₈H₄₀O₈, (I), see Fig. 1, is a derivative of *myo*-inositol. Upon heating, the crystalline substance passes a phase transition at about $T = 70^\circ\text{C}$, which is accompanied by vigorous mechanical jumps: if the needle-shaped crystals are not fixed in some way, they hop several cm high. This effect led to the laboratory jargon 'jumping crystals', and as a more serious characterization the term 'thermosalient solid' was coined (Gigg, Gigg, Payne & Conant, 1987). Upon cooling, the phase transition occurs at $T = 40^\circ\text{C}$, again with 'jumping'. In a calorimetric study, a second reversible phase transition was found at $T = 30^\circ\text{C}$ when heating and at $T = 11^\circ\text{C}$ when cooling, and the corresponding transition enthalpies were measured (Kohne, Praefcke & Mann, 1988). After melting at $T = 106^\circ\text{C}$, (I) does not crystallize upon cooling, but solidifies as a glass and shows a glass transition at $T = 2.9^\circ\text{C}$ (Kohne, Praefcke & Mann, 1988). These results can be summarized in the two following schemes, with the three phases designated as forms I, II, III; phase-transition temperatures are given in $^\circ\text{C}$ and enthalpies in kJ mol^{-1} (upper numbers for left to right processes; lower numbers for right to left processes):



In a recent solid-state NMR study of (I), only very subtle differences between the spectra of the crystalline phases were observed (Fattah, Twyman & Dobson, 1992).

Thermosalient behaviour has also been observed for crystals of other compounds. Examples are *ttatt*-perhydropyrene (Kohne, Praefcke & Mann, 1988; Ding, Herbst, Praefcke, Kohne & Saenger, 1991) and (phenylazophenyl)palladium hexafluoroacetylaceto-

nate (Etter & Siedle, 1983). In the former, rapid sublimation prevented crystallographic characterization of the high-temperature phase, and in the latter, the phase transition is irreversible. We suppose that thermosalient behaviour is exhibited by many more substances and often, although known, is not reported in structure communications [as is the case for MnCoGe, which has transition temperatures of 340 and 305 K on heating and cooling, respectively (Jeitschko, 1975) and crystals which jump up to 30 cm in the phase transition (Jeitschko, 1988)].

In a previous conference contribution on (I) (Steiner, Hinrichs, Gigg & Saenger, 1988), we have communicated the determination of the crystal structures of the forms II and III; in this paper we report the crystal structures of the three phases and some additional crystallographic observations.

Experimental

General observations

The synthesis of (I) was described by Gigg, Gigg, Payne & Conant (1987). Needle-shaped single crystals of form II were grown by slow evaporation of ethanolic solutions. If the evaporation is sufficiently slow, crystals of dimensions $\sim 30 \times 0.5 \times 0.3$ mm can be obtained. Under the polarizing microscope, the crystals have a fibrous appearance; this is in agreement with observations reported in the original paper 'that they may be in the form of a bundle of parallel fibres or leaves' (Gigg, Gigg, Payne & Conant, 1987).

Crystals were glued at one end to glass fibres and heated under the microscope. The sudden transition 'jump' was always initiated at one end of the crystal, followed by a transition front moving quickly along the needle axis to the other end within ~ 0.1 s. The transition front was accompanied by a sharp kink of several degrees in the crystal, and the needle length reduced by over 10%. These mechanical reactions certainly cause 'hopping' of the crystals, if they are not fixed. When cooled again, the transition occurred in reverse, leading to crystals of the original length. When the transitions were repeated several times, the crystals turned more opaque, and the fibrous appearance increased in each cycle, tiny fibres started to break off and after about 10–20 heating-cooling cycles the crystals looked rather like a truss of straw and disintegrated more and more into small particles.

Temperature dependence of the unit-cell parameters

For the crystallographic experiments, fragments ~ 0.5 mm long were cut out of the central parts of large crystals. The temperature dependence of the unit-cell constants of forms II and III was determined on a Stoe four-circle X-ray diffractom-

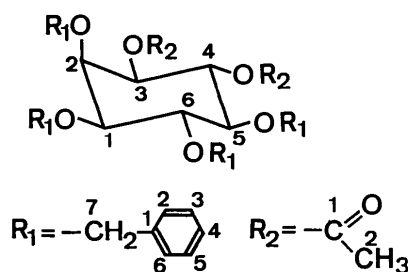


Fig. 1. Chemical formula and atom numbering of 3,4-di-*O*-acetyl-1,2,5,6-tetra-*O*-benzyl-*myo*-inositol. The O atom bound to C2 is axial with respect to the inositol ring, all others are equatorial.

eter (Ni-filtered Cu $K\alpha$ radiation) employing an Enraf–Nonius crystal-heating device, in which the crystal is bathed in a flow of hot air. The temperature was increased in steps of 5 or 10 °C from 18 to 90 °C; at each step, after allowing equilibration for ca 30 min, the unit-cell constants were determined from the setting angles of 20 reflections in the range $35 < 2\theta < 65^\circ$. In this experiment, the same crystal was used for the measurement of form II and, after passing the phase transition, for form III. As the heating device allows temperature measurement with only limited reliability, we expect the temperature only to be within $\pm 3^\circ\text{C}$ of that indicated on the thermometer. For form I, no corresponding measurements were made, as no suitable cooling–heating device was available in our laboratory.

Data collection

All crystal forms diffracted X-rays strongly, but the reflections were unusually broad. Several crystals from different crystallization batches and of different sizes were mounted, but no specimen with sharp reflections could be found. This may be caused by very large mosaic spread of the crystals (presumably associated with the fibrous macroscopic appearance), and is associated with systematic errors in measurements of both reflection and background intensities. Diffraction data sets were collected for form I at $T = 18^\circ\text{C}$, for form II at $T = 18$ and 60°C , and for form III at $T = 80^\circ\text{C}$. New crystals of size $\sim 0.5 \times 0.4 \times 0.1$ mm were used for each measurement [diffractometer as described above, ω – 2θ scan mode, background measurements on both sides of each scan, absorption correction using the ψ -scan method of North, Phillips & Matthews (1968)]. The crystal of form I was obtained by storing a mounted crystal of form II overnight in a freezer at 4°C , and the crystal of form III was obtained by heating a crystal of form II beyond the phase transition. Cell parameters were determined as described above; the crystallographic data are listed in Table 1. As a result of the loss of quality of the diffraction pattern, the crystals were not suitable for data collection after having traversed phase transitions more than once.

Structure solution and refinement

The crystal structures were solved by direct methods (Sheldrick, 1985) and refined with the program *SHELX76* (Sheldrick, 1976); the function minimized was $\sum w(|F_o| - |F_c|)^2$ with $w = 1$ for reflections with $F_o > \sigma(F_o)$. Owing to unacceptably poor positional refinement, the atoms of benzene rings 5A, 6A, 5B and 6B in form I, and of all benzene rings in form II had to be fixed in ideal geometry. In form II, no geometric constraints were necessary. In the final stages of anisotropic refinement, the H atoms were placed in their ideal calculated positions

Table 1. Crystallographic data for the 'jumping crystal' with *e.s.d.*'s in parentheses

Space group	Form I (18 °C)	Form II (18 °C)	Form II (60 °C)	Form III (80 °C)
	$P2_1/n$	$P2_1/c$	$P2_1/c$	$P2_1/c$
Z^*	8	4	4	4
a (Å)	28.883 (3)	14.269 (2)	14.464 (6)	16.241 (8)
b (Å)	15.189 (2)	14.862 (2)	14.923 (5)	15.230 (8)
c (Å)	15.566 (2)	16.506 (3)	16.385 (6)	14.385 (7)
β (°)	100.37 (1)	103.21 (1)	102.73 (3)	96.73 (4)
V (Å ³)	6717 (1)	3408 (1)	3450 (2)	3534 (3)
Calculated density (g cm ⁻³)	1.236	1.218	1.203	1.173
μ (cm ⁻¹)	6.63	6.54	6.46	6.30
$F(000)$	2656	1328	1328	1328
No. of unique reflections	8430	4510	3523	2993
No. of reflections	5788	3505	2338	1651
$F > \sigma(F)$				
Resolution† (Å)	0.9	0.9	1.0	1.1
R factor‡	0.090	0.086	0.093	0.083

* Number of molecules in the unit cell.

† Resolution = $\lambda/2 \sin \theta_{\text{max}}$.

‡ $R = \sum ||F_o| - |F_c|| / \sum |F_o|$ for the reflections with $F > \sigma(F)$.

[based on the shortened X-ray bond length of C—H, 0.98 Å (Allen, 1986)] except for constrained benzyl rings.

For the benzyl group (5) of molecule *B*, form I, apparent disorder was observed: the thermal parameters of C(1)5, C(2)5 and especially C(7)5 are particularly large, and substantial difference density peaks were observed in the vicinity of these atoms. This is indicative of crystallographic disorder. Several attempts to split these atomic sites (or the complete site of the constrained benzyl group) into two or more partially occupied alternative sites remained unsatisfactory. This might be as a result of the limit of crystallographic resolution (~ 1.0 Å), but could also indicate 'continuous' disorder. As an expedient, the benzyl ring was finally treated as an ideal hexagon with fully occupied atomic sites. This resulted in a stereochemically very poor covalent bond between C(1)5 and C(7)5. These problems could not be overcome with the available quality of data; in consequence the geometry of ring 5A of form I is not suitable for stereochemical analysis.

Refinements finally converged with R values of 0.090 (form I), 0.086 (form II, $T = 18^\circ\text{C}$), 0.093 (form II, $T = 60^\circ\text{C}$) and 0.083 (form III, $T = 80^\circ\text{C}$).

Results

General

For the four crystal structures of (I), final fractional coordinates of all non-H atoms and their equivalent isotropic temperature factors are given in Table 2, and atom labelling is shown in Fig. 1.*

* Lists of structure factors, anisotropic thermal parameters, bond lengths, bond angles, torsion angles and H-atom parameters have been deposited with the British Library Document Supply Centre as Supplementary Publication No. SUP 55921 (110 pp.). Copies may be obtained through The Technical Editor, International Union of Crystallography, 5 Abbey Square, Chester CH1 2HU, England. [CIF reference: SH0026]

Table 2. Fractional atomic coordinates and equivalent isotropic temperature factors (\AA^2) with e.s.d.'s in parentheses
$$U_{\text{eq}} = (1/3)[U_{22} + 1/\sin^2\beta(U_{11} + U_{33} + 2U_{13}\cos\beta)].$$

Form I, $T = 18^\circ\text{C}$		x	y	z	U_{eq}	Form II, $T = 18^\circ\text{C}$			
C1.4	0.1528 (2)	0.2746 (4)	0.2545 (4)	0.096 (8)	C(3)5B	0.6915 (3)	-0.1449 (3)	0.6861 (7)	0.15 (1)
C2.4	0.1757 (2)	0.3613 (4)	0.2895 (4)	0.098 (8)	C(4)5B	0.6499 (3)	-0.1762 (3)	0.6355 (7)	0.16 (1)
C3.4	0.2194 (2)	0.3392 (4)	0.3571 (4)	0.099 (8)	C(5)5B	0.6311 (3)	-0.1347 (3)	0.5570 (7)	0.17 (2)
C4.4	0.2056 (2)	0.2879 (4)	0.4319 (4)	0.096 (8)	C(6)5B	0.6539 (3)	-0.0618 (3)	0.5292 (7)	0.23 (2)
C5.4	0.1802 (2)	0.2033 (4)	0.3972 (4)	0.100 (8)	C(7)5B	0.6922 (6)	0.0257 (8)	0.495 (1)	0.52 (3)
C6.4	0.1375 (2)	0.2223 (4)	0.3266 (4)	0.097 (8)	C(1)6B	0.5750 (2)	-0.0388 (2)	0.2846 (3)	0.100 (8)
O1.4	0.1117 (2)	0.2902 (3)	0.1901 (3)	0.103 (6)	C(2)6B	0.6029 (2)	-0.0879 (2)	0.2379 (3)	0.12 (1)
O2.4	0.1457 (2)	0.4127 (3)	0.3318 (3)	0.106 (6)	C(3)6B	0.5975 (2)	-0.1791 (2)	0.2315 (3)	0.13 (1)
O3.4	0.2414 (2)	0.4202 (3)	0.3929 (3)	0.116 (6)	C(4)6B	0.5642 (2)	-0.2211 (2)	0.2719 (3)	0.12 (1)
O4.4	0.2494 (2)	0.2613 (3)	0.4871 (3)	0.108 (6)	C(5)6B	0.5363 (2)	-0.1720 (2)	0.3187 (3)	0.13 (1)
O5.4	0.1669 (2)	0.1588 (3)	0.4699 (3)	0.107 (6)	C(6)6B	0.5417 (2)	-0.0808 (2)	0.3250 (3)	0.12 (1)
O6.4	0.1206 (2)	0.1378 (3)	0.2953 (3)	0.114 (6)	C(7)6B	0.5812 (2)	0.0596 (4)	0.2936 (5)	0.12 (1)
C(1)1.4	0.0762 (3)	0.2975 (7)	0.0407 (5)	0.12 (1)	Form II, $T = 18^\circ\text{C}$				
C(2)1.4	0.0610 (4)	0.2287 (6)	-0.0139 (7)	0.14 (1)	C1	0.3227 (4)	0.2482 (4)	0.2787 (3)	0.102 (5)
C(3)1.4	0.0209 (4)	0.2333 (7)	-0.0755 (7)	0.16 (1)	C2	0.3706 (4)	0.3344 (4)	0.3178 (3)	0.106 (6)
C(4)1.4	-0.0057 (3)	0.3074 (7)	-0.0849 (5)	0.13 (1)	C3	0.4587 (4)	0.3104 (3)	0.3834 (3)	0.102 (5)
C(5)1.4	0.0083 (3)	0.3770 (6)	-0.0308 (6)	0.14 (1)	C4	0.4335 (4)	0.2545 (3)	0.4524 (3)	0.098 (5)
C(6)1.4	0.0489 (3)	0.3720 (6)	0.0294 (6)	0.13 (1)	C5	0.3773 (4)	0.1714 (3)	0.4169 (3)	0.102 (5)
C(7)1.4	0.1211 (3)	0.2928 (7)	0.1048 (5)	0.16 (1)	C6	0.2929 (4)	0.1899 (4)	0.3450 (3)	0.106 (5)
C(1)2.4	0.1007 (3)	0.5435 (5)	0.3320 (5)	0.105 (9)	O1	0.2397 (3)	0.2645 (3)	0.2138 (2)	0.113 (4)
C(2)2.4	0.0555 (3)	0.5740 (5)	0.3211 (6)	0.13 (1)	O2	0.3088 (3)	0.3847 (2)	0.3575 (2)	0.112 (4)
C(3)2.4	0.0426 (3)	0.6410 (6)	0.3719 (7)	0.15 (1)	O3	0.5067 (3)	0.3908 (2)	0.4204 (2)	0.114 (4)
C(4)2.4	0.0761 (4)	0.6773 (6)	0.4359 (7)	0.15 (1)	O4	0.5215 (3)	0.2249 (3)	0.5060 (3)	0.109 (4)
C(5)2.4	0.1211 (3)	0.6481 (6)	0.4455 (6)	0.15 (1)	O5	0.3495 (3)	0.1288 (2)	0.4843 (2)	0.120 (4)
C(6)2.4	0.1335 (3)	0.5822 (6)	0.3940 (6)	0.14 (1)	O6	0.2600 (3)	0.1050 (2)	0.3090 (2)	0.113 (4)
C(7)2.4	0.1146 (3)	0.4702 (5)	0.2785 (5)	0.13 (1)	C(1)1	0.1749 (5)	0.2785 (6)	0.0712 (5)	0.138 (6)
C(1)3.4	0.2751 (3)	0.4527 (6)	0.3553 (6)	0.13 (1)	C(2)1	0.1438 (6)	0.2170 (6)	0.0096 (5)	0.158 (7)
O(1)3.4	0.2890 (2)	0.4174 (4)	0.2974 (5)	0.18 (1)	C(3)1	0.0633 (6)	0.2301 (6)	-0.0542 (5)	0.161 (7)
C(2)3.4	0.2918 (3)	0.5413 (5)	0.3904 (5)	0.15 (1)	C(4)1	0.0106 (6)	0.3062 (6)	-0.0564 (5)	0.163 (7)
C(1)4.4	0.2537 (3)	0.2707 (5)	0.5747 (5)	0.11 (1)	C(5)1	0.0389 (7)	0.3684 (6)	0.0032 (6)	0.177 (7)
O(1)4.4	0.2243 (2)	0.3044 (4)	0.6091 (3)	0.139 (8)	C(6)1	0.1211 (6)	0.3549 (7)	0.0653 (5)	0.173 (7)
C(2)4.4	0.2990 (3)	0.2332 (5)	0.6204 (5)	0.14 (1)	C(7)1	0.2623 (5)	0.2706 (7)	0.1361 (4)	0.195 (7)
C(1)5.4	0.1649 (3)	0.0212 (4)	0.5427 (5)	0.13 (1)	C(1)2	0.2043 (6)	0.5106 (5)	0.3556 (4)	0.124 (6)
C(2)5.4	0.1968 (3)	0.0100 (4)	0.6207 (5)	0.18 (2)	C(2)2	0.1111 (7)	0.5057 (6)	0.3623 (5)	0.167 (7)
C(3)5.4	0.1861 (3)	-0.0471 (4)	0.6845 (5)	0.27 (2)	C(3)2	0.0751 (6)	0.5694 (8)	0.4106 (6)	0.202 (8)
C(4)5.4	0.1435 (3)	-0.0930 (4)	0.6703 (5)	0.35 (2)	C(4)2	0.1352 (8)	0.6339 (6)	0.4503 (6)	0.187 (7)
C(5)5.4	0.1117 (3)	-0.0818 (4)	0.5923 (5)	0.29 (2)	C(5)2	0.2272 (8)	0.6383 (6)	0.4439 (6)	0.184 (7)
C(6)5.4	0.1224 (3)	-0.0247 (4)	0.5285 (5)	0.19 (2)	C(6)2	0.2622 (6)	0.5780 (5)	0.3971 (5)	0.160 (7)
C(7)5.4	0.1762 (5)	0.0719 (6)	0.4720 (7)	0.28 (2)	C(7)2	0.2452 (6)	0.4448 (5)	0.3041 (5)	0.180 (7)
C(1)6.4	0.0553 (2)	0.0420 (4)	0.2813 (4)	0.13 (1)	C(1)3	0.5728 (5)	0.4250 (4)	0.3859 (4)	0.113 (6)
C(2)6.4	0.0757 (2)	-0.0348 (4)	0.2563 (4)	0.16 (1)	O(1)3	0.5980 (4)	0.3901 (3)	0.3295 (3)	0.193 (6)
C(3)6.4	0.0589 (2)	-0.1168 (4)	0.2770 (4)	0.17 (2)	C(2)3	0.6101 (5)	0.5144 (4)	0.4221 (4)	0.140 (6)
C(4)6.4	0.0217 (2)	-0.1219 (4)	0.3227 (4)	0.17 (2)	C(1)4	0.5356 (5)	0.2387 (4)	0.5875 (4)	0.108 (6)
C(5)6.4	0.0012 (2)	-0.0451 (4)	0.3477 (4)	0.17 (1)	O(1)4	0.4807 (3)	0.2813 (3)	0.6193 (3)	0.144 (5)
C(6)6.4	0.0180 (2)	0.0369 (4)	0.3270 (4)	0.15 (1)	C(2)4	0.6248 (5)	0.1948 (4)	0.6358 (4)	0.137 (6)
C(7)6.4	0.0723 (3)	0.1312 (5)	0.2632 (6)	0.14 (1)	C(1)5	0.3472 (6)	-0.0133 (4)	0.5541 (4)	0.131 (6)
C1B	0.6529 (2)	0.2259 (4)	0.2703 (4)	0.089 (8)	C(2)5	0.4192 (7)	0.0056 (6)	0.6142 (6)	0.168 (7)
C2B	0.6755 (2)	0.3112 (4)	0.3098 (4)	0.095 (8)	C(3)5	0.4419 (7)	-0.0451 (6)	0.6831 (6)	0.184 (7)
C3B	0.7217 (2)	0.2879 (4)	0.3680 (4)	0.093 (8)	C(4)5	0.3860 (8)	-0.1144 (6)	0.6921 (6)	0.202 (7)
C4B	0.7131 (2)	0.2314 (4)	0.4426 (4)	0.088 (7)	C(5)5	0.3027 (8)	-0.1359 (6)	0.6337 (8)	0.221 (8)
C5B	0.6884 (2)	0.1464 (4)	0.4074 (4)	0.097 (8)	C(6)5	0.2836 (6)	-0.0830 (5)	0.5584 (5)	0.164 (7)
C6B	0.6432 (2)	0.1641 (4)	0.3400 (4)	0.090 (8)	C(7)5	0.3310 (9)	0.0381 (5)	0.4746 (5)	0.256 (7)
O1B	0.6091 (2)	0.2411 (3)	0.105 (6)	0.105 (6)	C(1)6	0.1409 (5)	-0.0079 (4)	0.2753 (5)	0.125 (6)
O2B	0.6475 (2)	0.3567 (3)	0.3613 (3)	0.100 (5)	C(2)6	0.1794 (5)	-0.0543 (5)	0.2185 (5)	0.144 (6)
O3B	0.7447 (2)	0.3677 (3)	0.4052 (3)	0.107 (6)	C(3)6	0.1645 (6)	-0.1453 (5)	0.2083 (5)	0.157 (7)
O4B	0.7588 (2)	0.2046 (3)	0.4903 (3)	0.105 (6)	C(4)6	0.1109 (5)	-0.1900 (5)	0.2554 (5)	0.139 (7)
O5B	0.6767 (2)	0.0989 (3)	0.4779 (3)	0.104 (5)	C(5)6	0.0715 (6)	-0.1454 (5)	0.3117 (5)	0.157 (7)
O6B	0.6295 (2)	0.0801 (3)	0.3028 (3)	0.105 (6)	C(6)6	0.0872 (5)	-0.0532 (5)	0.3219 (5)	0.147 (7)
C(1)1B	0.5805 (3)	0.2242 (5)	0.0618 (5)	0.098 (9)	C(7)6	0.1594 (5)	0.0936 (4)	0.2892 (5)	0.152 (6)
C(2)1B	0.5846 (3)	0.1333 (6)	0.0591 (6)	0.13 (1)	Form II, $T = 60^\circ\text{C}$				
C(3)1B	0.5551 (4)	0.0880 (6)	-0.0062 (7)	0.16 (1)	C1	0.3236 (7)	0.2470 (6)	0.2766 (6)	0.13 (1)
C(4)1B	0.5227 (3)	0.1300 (8)	-0.0665 (6)	0.15 (1)	C2	0.3698 (7)	0.3346 (6)	0.3166 (6)	0.13 (1)
C(5)1B	0.5185 (3)	0.2189 (7)	-0.0637 (6)	0.14 (1)	C3	0.4564 (7)	0.3098 (6)	0.3787 (6)	0.13 (1)
C(6)1B	0.5481 (3)	0.2651 (6)	-0.0003 (5)	0.12 (1)	C4	0.4311 (7)	0.2543 (6)	0.4505 (6)	0.12 (1)
C(7)1B	0.6126 (3)	0.2747 (5)	0.1288 (4)	0.12 (1)	C5	0.3790 (7)	0.1704 (6)	0.4144 (6)	0.12 (1)
C(1)2B	0.6002 (3)	0.4845 (5)	0.3733 (5)	0.11 (1)	C6	0.2923 (7)	0.1903 (6)	0.3452 (6)	0.13 (1)
C(2)2B	0.5548 (3)	0.5014 (5)	0.3805 (6)	0.13 (1)	O1	0.2389 (5)	0.2639 (4)	0.2131 (4)	0.141 (8)
C(3)2B	0.5452 (3)	0.5692 (7)	0.4344 (7)	0.16 (1)	O2	0.3075 (5)	0.3829 (4)	0.3558 (4)	0.138 (8)
C(4)2B	0.5801 (4)	0.6209 (6)	0.4771 (6)	0.15 (1)	O3	0.5020 (5)	0.3905 (4)	0.4167 (4)	0.143 (8)
C(5)2B	0.6262 (4)	0.6047 (6)	0.4690 (6)	0.15 (1)	O4	0.5199 (5)	0.2264 (4)	0.5035 (5)	0.137 (8)
C(6)2B	0.6358 (3)	0.5371 (6)	0.4167 (6)	0.14 (1)	O5	0.3494 (5)	0.1294 (4)	0.4832 (4)	0.145 (8)
C(7)2B	0.6109 (3)	0.4116 (5)	0.3158 (5)	0.12 (1)	O6	0.2608 (5)	0.1047 (4)	0.3082 (4)	0.141 (8)
C(1)3B	0.7737 (3)	0.4064 (6)	0.3631 (7)	0.14 (1)	C(1)1	0.176 (1)	0.275 (1)	0.0693 (9)	0.18 (1)
O(1)3B	0.7827 (3)	0.3785 (5)	0.2967 (5)	0.24 (1)	C(2)1	0.143 (1)	0.2145 (9)	0.0067 (9)	0.20 (1)
C(2)3B	0.7931 (3)	0.4904 (5)	0.4019 (5)	0.15 (1)	C(3)1	0.061 (1)	0.233 (1)	-0.0543 (8)	0.20 (1)
C(1)4B	0.7679 (3)	0.2156 (5)	0.5782 (5)	0.100 (9)	C(4)1	0.012 (1)	0.311 (1)	-0.0546 (8)	0.20 (1)
O(1)4B	0.7409 (2)	0.2516 (3)	0.6172 (3)	0.129 (7)	C(5)1	0.045 (1)	0.3689 (9)	0.008 (1)	0.23 (2)
C(2)4B	0.8135 (2)	0.1762 (5)	0.6179 (5)	0.13 (1)	C(6)1	0.125 (1)	0.350 (1)	0.0673 (9)	0.22 (2)
C(1)5B	0.6954 (3)	-0.0305 (3)	0.5798 (7)	0.24 (2)					
C(2)5B	0.7142 (3)	-0.0721 (3)	0.6582 (7)	0.17 (1)					

Table 2 (cont.)

	<i>x</i>	<i>y</i>	<i>z</i>	<i>U_{eq}</i>		<i>x</i>	<i>y</i>	<i>z</i>	<i>U_{eq}</i>
C(7)1	0.2654 (9)	0.267 (1)	0.1333 (7)	0.23 (1)	O3	0.4559 (5)	0.3866 (6)	0.3614 (5)	0.19 (1)
C(1)2	0.204 (1)	0.5077 (8)	0.3535 (8)	0.16 (1)	O4	0.4862 (6)	0.2311 (5)	0.4521 (6)	0.18 (1)
C(2)2	0.115 (1)	0.503 (1)	0.3594 (9)	0.22 (2)	O5	0.3464 (5)	0.1199 (5)	0.4569 (5)	0.19 (1)
C(3)2	0.076 (1)	0.563 (2)	0.410 (1)	0.27 (2)	O6	0.2645 (5)	0.0960 (6)	0.2773 (6)	0.20 (1)
C(4)2	0.133 (2)	0.631 (1)	0.445 (1)	0.25 (2)	C(1)1	0.1461 (4)	0.2713 (8)	0.0261 (5)	0.20 (1)
C(5)2	0.225 (1)	0.632 (1)	0.446 (1)	0.23 (2)	C(2)1	0.1069 (4)	0.2060 (8)	-0.0309 (5)	0.23 (2)
C(6)2	0.258 (1)	0.573 (1)	0.3960 (9)	0.20 (1)	C(3)1	0.0318 (4)	0.2237 (8)	-0.0852 (5)	0.26 (2)
C(7)2	0.247 (1)	0.4443 (8)	0.3040 (7)	0.24 (1)	C(4)1	-0.0041 (4)	0.3067 (8)	-0.0825 (5)	0.26 (2)
C(1)3	0.5680 (8)	0.4219 (7)	0.3818 (7)	0.15 (1)	C(5)1	0.0351 (4)	0.3720 (8)	-0.0254 (5)	0.26 (2)
O(1)3	0.5939 (6)	0.3882 (5)	0.3255 (6)	0.22 (1)	C(6)1	0.1102 (4)	0.3543 (8)	0.0289 (5)	0.26 (2)
C(2)3	0.6038 (7)	0.5134 (6)	0.4215 (6)	0.18 (1)	C(7)1	0.2242 (8)	0.253 (1)	0.0761 (8)	0.28 (2)
C(1)4	0.5321 (9)	0.2396 (7)	0.5855 (7)	0.14 (1)	C(1)2	0.2071 (7)	0.4922 (5)	0.3583 (6)	0.21 (1)
O(1)4	0.4782 (6)	0.2801 (5)	0.6184 (4)	0.17 (1)	C(2)2	0.1228 (7)	0.5119 (5)	0.3424 (6)	0.29 (2)
C(2)4	0.6223 (7)	0.1956 (7)	0.6324 (6)	0.17 (1)	C(3)2	0.0876 (7)	0.5698 (5)	0.4018 (6)	0.32 (2)
C(1)5	0.351 (1)	-0.0111 (7)	0.5559 (8)	0.17 (1)	C(4)2	0.1369 (7)	0.6080 (5)	0.4770 (6)	0.34 (2)
C(2)5	0.423 (1)	0.002 (1)	0.618 (1)	0.24 (2)	C(5)2	0.2212 (7)	0.5883 (5)	0.4929 (6)	0.36 (2)
C(3)5	0.437 (1)	-0.054 (1)	0.6844 (9)	0.27 (2)	C(6)2	0.2564 (7)	0.5304 (5)	0.4335 (6)	0.29 (2)
C(4)5	0.371 (2)	-0.121 (1)	0.682 (1)	0.30 (2)	C(7)2	0.2320 (9)	0.431 (1)	0.2866 (9)	0.28 (2)
C(5)5	0.291 (2)	-0.131 (1)	0.623 (2)	0.33 (2)	C(1)3	0.520 (1)	0.422 (1)	0.329 (1)	0.22 (2)
C(6)5	0.289 (1)	-0.076 (1)	0.5552 (8)	0.21 (2)	O(1)3	0.5447 (6)	0.3886 (7)	0.2606 (8)	0.35 (1)
C(7)5	0.343 (2)	0.0389 (8)	0.4774 (9)	0.39 (2)	C(2)3	0.5563 (8)	0.5048 (8)	0.3737 (8)	0.26 (2)
C(1)6	0.1439 (8)	-0.0086 (7)	0.2757 (7)	0.15 (1)	C(1)4	0.5075 (9)	0.2542 (9)	0.542 (1)	0.18 (1)
C(2)6	0.1840 (8)	-0.0544 (8)	0.2204 (8)	0.18 (1)	O(1)4	0.4590 (6)	0.2883 (6)	0.5896 (5)	0.23 (1)
C(3)6	0.1683 (9)	-0.1463 (9)	0.2101 (8)	0.19 (1)	C(2)4	0.5956 (7)	0.2327 (8)	0.5797 (7)	0.21 (1)
C(4)6	0.1134 (9)	-0.1883 (7)	0.2574 (8)	0.16 (1)	C(1)5	0.3490 (7)	-0.0137 (5)	0.5396 (6)	0.19 (1)
C(5)6	0.071 (1)	-0.1447 (9)	0.3188 (8)	0.20 (1)	C(2)5	0.3963 (7)	-0.0454 (5)	0.6198 (6)	0.23 (1)
C(6)6	0.0887 (9)	-0.0525 (9)	0.3214 (7)	0.18 (1)	C(3)5	0.3622 (7)	-0.1058 (5)	0.6773 (6)	0.32 (2)
C(7)6	0.1609 (8)	0.0938 (7)	0.2906 (8)	0.19 (1)	C(4)5	0.2808 (7)	-0.1346 (5)	0.6546 (6)	0.36 (2)
					C(5)5	0.2335 (7)	-0.1030 (5)	0.5744 (6)	0.31 (2)
Form III, <i>T</i> = 80 °C					C(6)5	0.2675 (7)	-0.0425 (5)	0.5169 (6)	0.25 (2)
C1	0.3026 (8)	0.2396 (9)	0.2330 (8)	0.16 (1)	C(7)5	0.3900 (9)	0.0437 (9)	0.477 (1)	0.27 (2)
C2	0.3373 (8)	0.3271 (9)	0.2663 (9)	0.18 (1)	C(1)6	0.1631 (7)	-0.0163 (5)	0.2740 (5)	0.18 (1)
C3	0.4205 (8)	0.3034 (8)	0.3228 (8)	0.17 (1)	C(2)6	0.2256 (7)	-0.0762 (5)	0.2608 (5)	0.23 (2)
C4	0.4048 (8)	0.2531 (9)	0.4067 (9)	0.17 (1)	C(3)6	0.2122 (7)	-0.1659 (5)	0.2714 (5)	0.27 (2)
C5	0.3648 (8)	0.1679 (9)	0.3770 (9)	0.18 (1)	C(4)6	0.1361 (7)	-0.1957 (5)	0.2952 (5)	0.27 (2)
C6	0.2855 (8)	0.1834 (9)	0.3117 (9)	0.18 (1)	C(5)6	0.0736 (7)	-0.1358 (5)	0.3084 (5)	0.27 (2)
O1	0.2243 (5)	0.2556 (5)	0.1765 (5)	0.19 (1)	C(6)6	0.0871 (7)	-0.0461 (5)	0.2978 (5)	0.25 (2)
O2	0.2885 (5)	0.3699 (5)	0.3276 (5)	0.19 (1)	C(7)6	0.1795 (8)	0.0786 (9)	0.2651 (9)	0.22 (2)

The crystals of forms II and III belong to the monoclinic centrosymmetric space group $P2_1/c$, with one molecule in the asymmetric unit and four molecules in the unit cell; solvent (ethanol) molecules did not cocrystallize. The unit-cell setting was chosen such that the *c* axis coincides with the crystal needle axis. Form I is monoclinic $P2_1/n$ with eight molecules in the unit cell and a cell volume about twice as large as forms II and III.

Temperature dependence of the unit-cell parameters

Table 1 and Fig. 2 show that the unit-cell constants change dramatically when the phase transitions take place; in the transition II→III, the *c* axis (= needle axis) reduces by 12%, the angle β reduces by 6°, and the volume per molecule increases by $\sim 17 \text{ \AA}^3$ ($\Delta V/V = 2.0\%$). This correlates with the observed changes of the macroscopic crystal geometry during the transition II→III, *i.e.* reduction of the needle length by over 10%, and a kink running with the transition front. This shows that the morphology of the crystals follows the sudden changes of the unit cell (as it must). The coefficient of thermal volume expansion $\alpha = 1/V(dV/dT)$ is larger for form II ($2.5 \times 10^{-4} \text{ }^\circ\text{C}^{-1}$) than for form III ($2.0 \times 10^{-4} \text{ }^\circ\text{C}^{-1}$, Fig. 2; estimated accuracy of the measurement around $\Delta\alpha \pm 0.1$ or $0.2 \times 10^{-4} \text{ }^\circ\text{C}^{-1}$); both values are in the range usually observed for organic

compounds with weak intermolecular forces [*e.g.* macroscopic $\alpha = 2.2 \times 10^{-4} \text{ }^\circ\text{C}^{-1}$ for anthracene, and $\alpha = 2.7 \times 10^{-4} \text{ }^\circ\text{C}^{-1}$ for naphthalene (D'Ans & Lax, 1967)].

For the transition I→II, the changes in unit-cell constants are less pronounced, but still substantial: *c* increases by $\sim 6\%$, β increases by 2.8° and the volume per molecule increases by $\sim 12 \text{ \AA}^3$, $\Delta V/V = 1.4\%$ (the halving of the *a* axis is associated with a halving of the unit-cell content).

The temperature dependence of the unit-cell constants for forms II and III shows a strong hysteresis effect (Fig. 2). If form II is heated slowly, the unit-cell constants change linearly in the same direction in which they change in the phase transition: the *a* and *b* axes gradually lengthen upon heating and also lengthen at the phase transition; the *c* axis and the angle β reduce upon heating, and consistently also reduce in the phase transition. This behaviour is not shown by form III: here *c* and β reduce upon cooling and increase in the phase transition, and *a* and *b* remain virtually constant upon cooling and are reduced in the transition.

Crystal packing

The crystal packing for the three crystal forms is shown in Fig. 3 in views down the monoclinic axis. The changes of the unit-cell constants *a*, *c* and β that

occur with the phase transitions are obvious. The main features of the arrangement are very similar in all crystal forms; apart from some conformational differences (see below), the molecules are shifted only slightly with respect to each other. The increase in unit-cell volume associated with the phase transition is not filled by a certain part of the molecule, but by the molecules as a whole as a result of subtle changes in conformation. Suspiciously short intermolecular (or intramolecular) contacts and interstitial cavities are not observed.

The molecular conformation

The molecular conformation is described by torsion angles (see the supplementary material) which can be studied qualitatively in Figs. 4–6. The inositol ring is in a chair conformation, and the ring torsion angles in all structures deviate only slightly from the ideal values of $\pm 60^\circ$.

The conformational changes of the benzyl and acetyl groups which occur during the phase transitions are shown in superposition diagrams in Fig. 6(a) for the transition I \leftrightarrow II, and Fig. 6(b) for II \leftrightarrow III. The flip angles of all relevant torsional parameters are listed in Table 3. Note that in the transition I \rightarrow II, the changes differ significantly for the two independent molecules of form I because their conformations have to converge at the same structure in form II.

For the acetyl groups, the flip angles are not larger than $\sim 10^\circ$; this is small compared with those of the phenyl groups.

The four benzyl C—O—CH₂—C₆H₅ groups have three bonds about which rotations may occur, and consequently they exhibit conformational flexibility. In all the crystal structures considered here, the benzyl groups (1), (5) and (6) are roughly in the

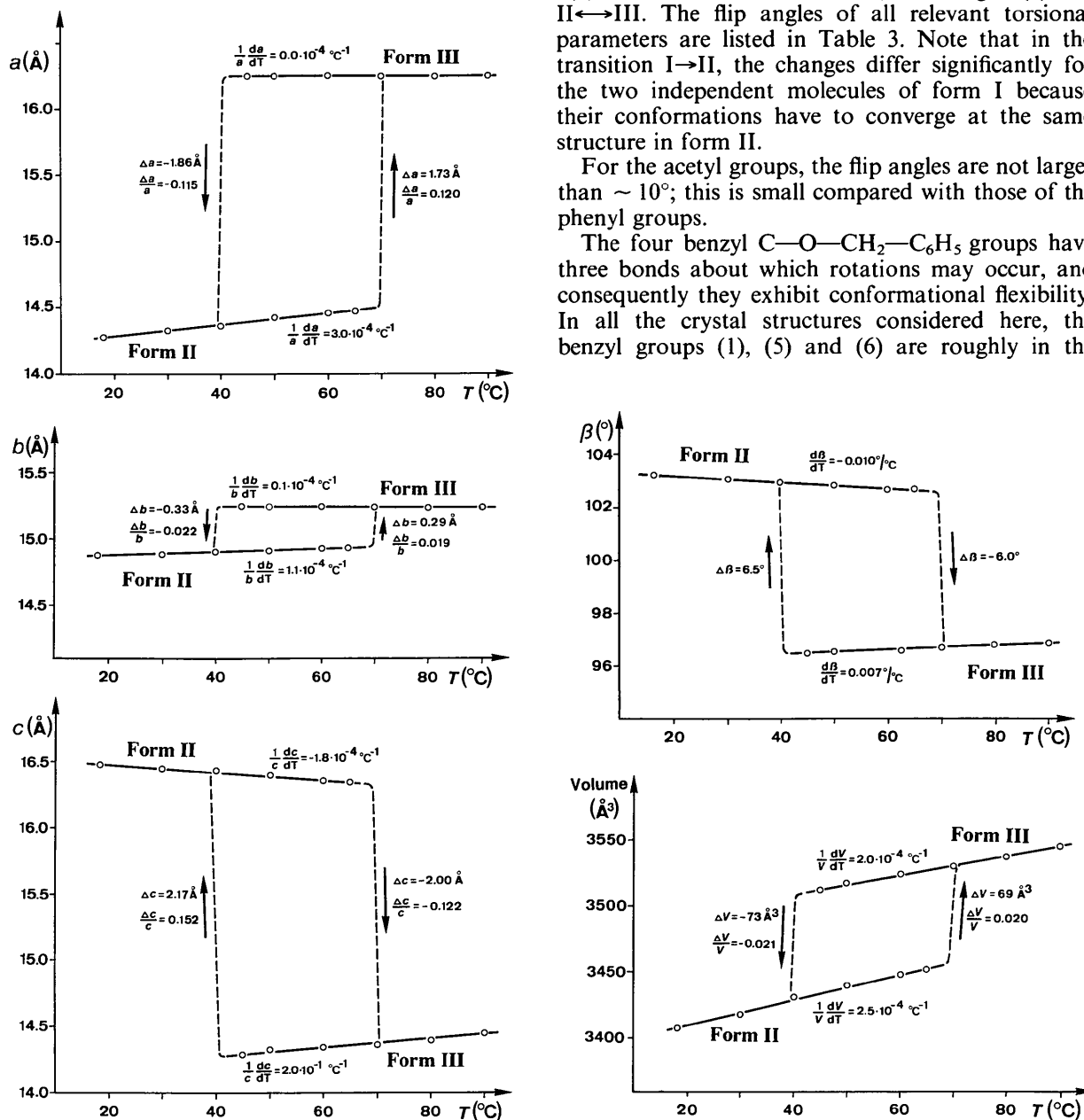


Fig. 2. Unit-cell constants a , b , c , β and V of crystal forms II and III as a function of temperature. The directionality of the phase transitions is indicated by arrows. Estimated accuracies of the coefficients of thermal expansion, $(1/a)(da/dT)$ etc. $\pm 0.1 \times 10^{-4} \text{ K}^{-1}$.

inositol plane, while (2) is perpendicular to it according to the axial orientation of O2, see Figs. 4 and 5.

Although the overall conformation of the molecules remains similar during the phase transitions, the benzyl groups perform significant movements. These are very complex, as all 'free' torsion angles of each group rotate with flip angles up to over 70° (Table 3). The largest movement is performed by group (5) in the transition II(60 °C)→III(80 °C), where the three torsion angles change by 37° around the bond C5—O5, by 41° around O5—C(7)5 and by -76° around C(7)5—C(1)1. Benzyl (5) is also the only group which substantially changes when form II is heated from 18 to 60 °C (Table 3). This flexibility of benzyl (5) might also be associated with the disorder observed in form I (see above).

Displacement parameters

The displacement parameters are unusually high in all four crystal structures: for the six C atoms of the inositol ring, which has a well defined geometry, the

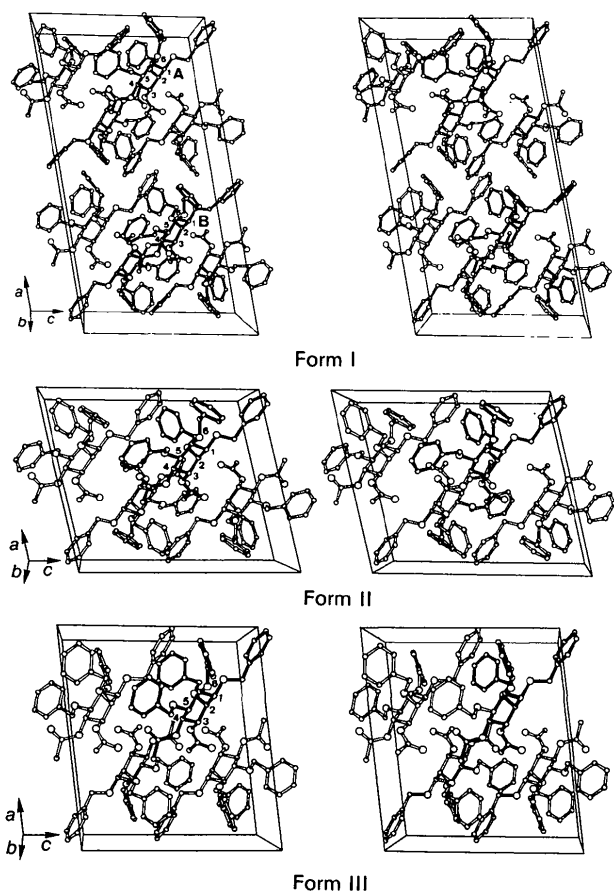


Fig. 3. Crystal packing of the jumping crystal for all three crystal forms shown in perspective stereoplots. Projections are down the monoclinic b axis. For clarity, one of the symmetry-independent molecules is drawn with filled bonds.

average values are $\langle U_{eq} \rangle = 0.098$ (8) and 0.092 (6) \AA^2 for form I (molecules *A* and *B*, respectively, at 18 °C), $\langle U_{eq} \rangle = 0.103$ (6) \AA^2 for form II (18 °C), $\langle U_{eq} \rangle = 0.126$ (7) \AA^2 for form II (60 °C), and $\langle U_{eq} \rangle = 0.17$ (1) \AA^2 for form III (80 °C) (r.m.s. deviations given in parentheses). At room temperature, the temperature factors are about two to three times larger than in 'well behaved' structures of small organic molecules. This may be as a result of several factors: it may in principle be caused by unusually strong thermal vibrations in the crystal; by some degree of crystallographic disorder; or it may be an artefact as a result of the strong mosaic spread or because of associated systematic errors in the meas-

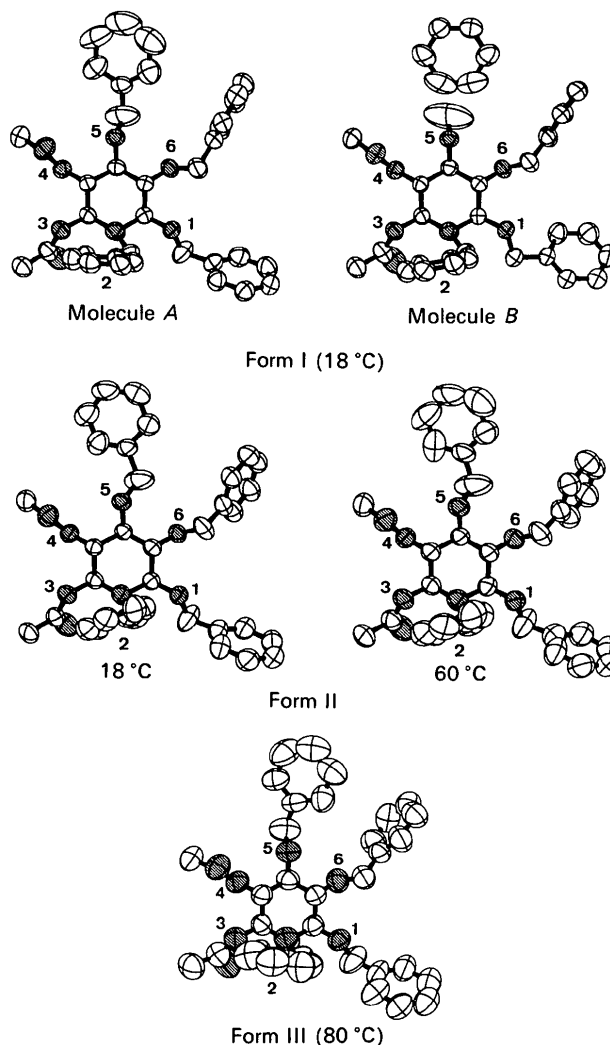


Fig. 4. Thermal ellipsoid plots (Johnson, 1976) of the molecules in each crystal form, 30% probability ellipsoids, O atoms are drawn shaded. In form I, molecule *B*, the benzyl group (5) is refined with poor geometry because of apparent disorder, resulting in poor covalent geometry of the bond C(7)5—C(1)5; therefore this bond is not drawn. Projections are on the plane formed by C1, C3 and C5 of the inositol ring.

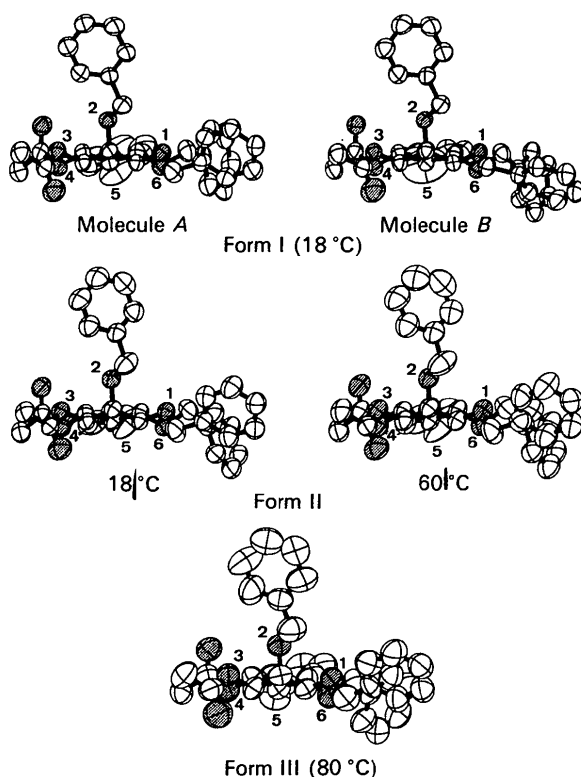


Fig. 5. As Fig. 4, projection perpendicular to the plane formed by C1, C3 and C5 of the inositol ring. Side groups are labelled at the O atom.

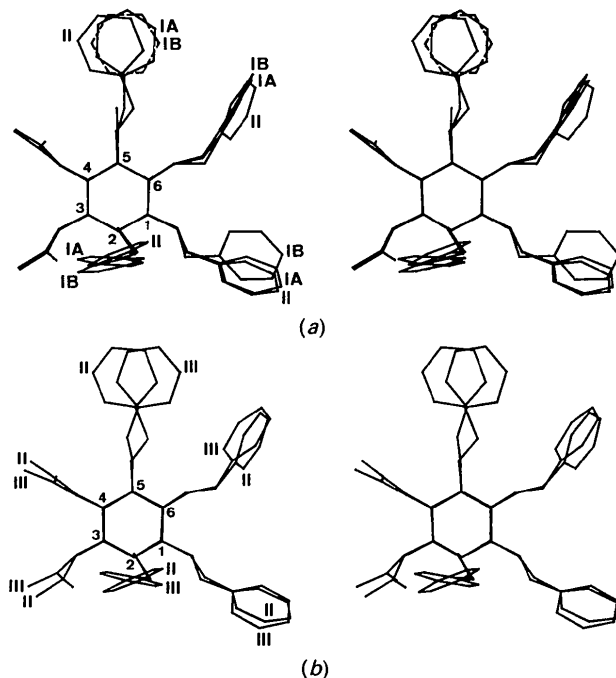


Fig. 6. Stereographic superposition plots of the molecules found (a) in forms I and II, and (b) in forms II and III. Benzyl group (5) of molecule IB is drawn dashed and without the bond C7—C1 because of disorder (as in Fig. 4).

Table 3. Differences of selected torsion angles ('flip angles' ($^{\circ}$)) in different phases of the 'jumping crystal'

	$I^A \rightarrow II^{18*}$	$I^B \rightarrow II^{18*}$	$II^{18} \rightarrow II^{60*}$	$II^{60} \rightarrow III^{80*}$
C6—C1—O1—C(7)1	0.4 (8)	14.0 (7)	-0.1 (9)	8 (1)
C1—O1—C(7)1—C(1)1	1.9 (8)	41.3 (8)	0 (1)	6 (1)
O1—C(7)1—C(1)1—C(2)1	-5 (1)	-61 (1)	-3 (1)	2 (1)
C1—C2—O2—C(7)2	1.0 (9)	-4.0 (9)	-2 (1)	-7 (1)
C2—O2—C(7)2—C(1)2	-8.2 (8)	-11.8 (8)	0 (1)	5 (1)
O2—C(7)2—C(1)2—C(2)2	31 (1)	24 (1)	2 (2)	-36 (2)
C2—C3—O3—C(1)3	2.9 (9)	0.7 (9)	-4 (1)	-14 (1)
C3—O3—C(1)3—C(2)3	-0.6 (8)	-2.9 (8)	1 (1)	9 (1)
C3—O3—C(1)3—O(1)3	0 (1)	-3 (1)	1 (2)	10 (2)
C3—C4—O4—C(1)4	-6.7 (8)	-1.5 (8)	2 (1)	-7 (1)
C4—O4—C(1)4—C(2)4	-2.0 (8)	-0.4 (7)	-1 (1)	12 (1)
C4—O4—C(1)4—O(1)4	-2 (1)	-1 (1)	-1 (2)	12 (3)
C4—C5—O5—C(7)5	-21.5 (9)	-37 (1)	6 (1)	37 (1)
C5—O5—C(7)5—C(1)5†	-26 (1)	—	4 (1)	41 (1)
O5—C(7)5—C(1)5—C(2)5†	50 (1)	—	-14 (1)	-76 (2)
C5—C6—O6—C(7)6	-14.6 (8)	0.9 (7)	2 (1)	5 (1)
C6—O6—C(7)6—C(1)6	-17.1 (8)	-4.2 (7)	0 (1)	12 (1)
O6—C(7)6—C(1)6—C(2)6	-2 (1)	-18 (1)	3 (1)	31 (1)

* Differences between the structures: I(molecule A)(18 °C)→II(18 °C), I(molecule B)(18 °C)→II(18 °C), II(18 °C)→II(60 °C) and II(60 °C)→III(80 °C).

† $I^B \rightarrow II^{18}$ not given due to apparent disorder.

urement of reflection intensities, which are known to mainly influence the thermal parameters.

As expected, the temperature factors become even larger for the atoms of the flexible substituents: in form II (18 °C), for example, $\langle U_{eq} \rangle = 0.113 (7) \text{ \AA}^2$ for the six inositol O atoms, $\langle U_{eq} \rangle = 0.14 (3) \text{ \AA}^2$ for the six atoms of the two acetyl groups, and $\langle U_{eq} \rangle = 0.17 (3) \text{ \AA}^2$ for the 28 atoms of the four benzyl groups, see also Fig. 4. Although the absolute values of the U_{eq} may be systematically too high, the relative behaviour indicates that the substituents are significantly more mobile than the central inositol moieties.

In Table 4, the thermal behaviour of the substituents is listed in more detail. It is evident that: (i) The mean temperature factor of the acetyl group (3) is always slightly higher than that of acetyl group (4). (ii) In form I, benzyl groups (1), (2) and (6) have similar temperature factors, while that of group (5) is significantly larger. In forms II and III, the benzyl groups have comparable U_{eq} in each of the crystal structures.

In Figs. 4 and 5 the thermal ellipsoids are drawn for all individual molecules in order to show the directionality of the anisotropic thermal motions.

C—H...O=C hydrogen bonds

The acetyl groups are placed in the region $x = 1/2$ in forms II, III, and in $x = 1/4$ and $x = 3/4$ in form I, see Fig. 3. Each acetyl O atom is in close contact with a methyl C atom of a neighbouring molecule, with $d_{O...C}$ between about 3.1 and 3.5 Å, a distance which suggests that C—H...O=C hydrogen bonds are present (Sutor, 1963; Taylor & Kennard, 1982; Desiraju, 1991). This layer-type arrangement is

Table 4. Mean equivalent isotropic temperature factors $\langle U_{eq} \rangle$ (\AA^2) of the substituent groups at different temperatures

For monoclinic space groups: $U_{eq} = (1/3)[U_{22} + 1/\sin^2\beta(U_{11} + U_{33} + 2U_{13}\cos\beta)]$. $\langle U_{eq} \rangle = (\sum_{i=1}^n U_{eq,i})/n$, the summation is over the n atoms of the group. R.m.s. deviations are given in parentheses: r.m.s. = $[\sum_{i=1}^n ((U_{eq,i} - \langle U_{eq} \rangle)^2 / (n-1))]^{1/2}$.

Form	Temp.	C (Inositol)	O (Inositol)	Acetyl (3)	Acetyl (4)	Benzyl (1)	Benzyl (2)	Benzyl (5)	Benzyl (6)
I ^a	18 °C	0.098 (8)	0.109 (8)	0.15 (3)	0.13 (2)	0.14 (1)	0.14 (2)	0.24 (8)	0.16 (2)
I ^b	18 °C	0.092 (6)	0.104 (5)	0.18 (6)	0.12 (2)	0.13 (2)	0.14 (2)	0.23 (12)	0.12 (1)
II	18 °C	0.103 (6)	0.113 (7)	0.15 (4)	0.13 (2)	0.17 (2)	0.17 (3)	0.19 (4)	0.15 (1)
II	60 °C	0.126 (7)	0.141 (7)	0.18 (4)	0.16 (2)	0.21 (2)	0.22 (4)	0.27 (8)	0.18 (2)
III	80 °C	0.17 (1)	0.190 (6)	0.28 (7)	0.21 (3)	0.25 (3)	0.30 (5)	0.28 (6)	0.24 (3)

shown in more detail in Fig. 7. The C...O distances become longer in the transition I→II and shorter in the transition II→III, but the general pattern is conserved. The stability of the pattern can be taken as an indication that it actually plays a role in stabilizing the structures.

We note that formalisms for descriptions of hydrogen-bond patterns are appropriate for C—H...O in the same way as for all other hydrogen bonds (also see Steiner & Saenger, 1992). In the formalism of Kuleshova & Zorky (1980) the pattern

of C—H...O=C hydrogen bonds described is denoted as the 'aggregate' $L_3^4(2,6)$, one of the more commonly observed patterns ('L' stands for 'layer'). In the graph-set analysis of Etter, MacDonald & Bernstein (1990) it is decoded into chains and rings of different 'orders', e.g. chains in the direction of the b axis near $z = 1/4$ and $3/4$ (Fig. 7) that are categorized as $C_2^2(8)$ or rings with the centre at $y = z = 1/2$, $R_2^2(18)$.

The arrangement of the hydrogen bonds is not affected by the change of space group in the transi-

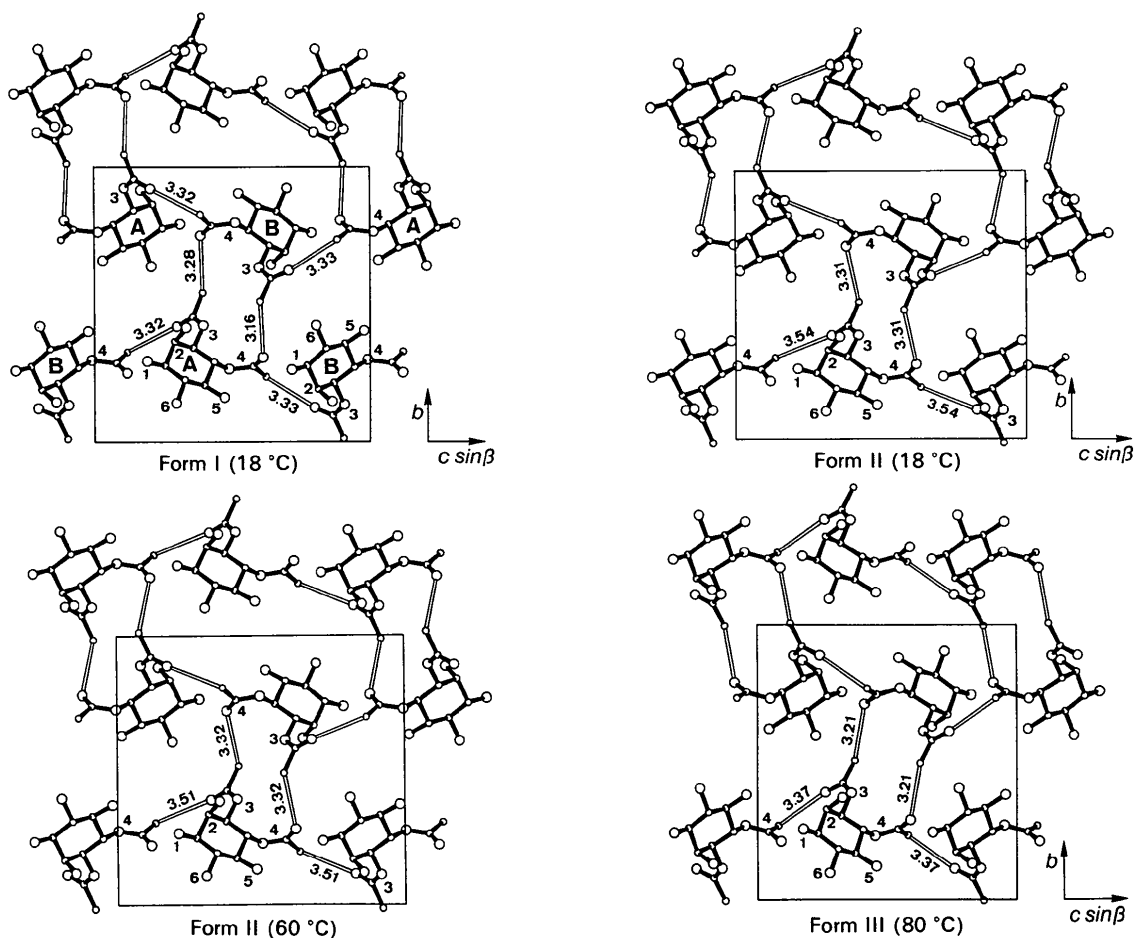


Fig. 7. Short C...O=C contacts of the acetyl groups that are indicative of C—H...O=C hydrogen bonds. Projections are along the a axes (distances in \AA). For form I, the section around $x = 1/4$ is drawn.

tion I→II; however, the internal symmetry of the pattern alters. For example, the two molecules that build the $R_2^2(18)$ ring are symmetry independent in form I, but symmetry related in forms II and III; consequently the two intermolecular hydrogen bonds of that ring are different in form I, and equivalent in forms II and III (Fig. 7). Similarly, the two $C_2^2(8)$ chains mentioned above are symmetry independent in form I, but equivalent in the other forms (Fig. 7).

The 'jumping' effect

The reason for the 'jumping' effect is not evident from the crystal structures. It is obvious from the increase/decrease of the unit-cell constants (Fig. 2) that upon heating form II becomes increasingly stressed, and at some point, this stress is released in a phase transition. All attempts to understand the reason for this behaviour on the basis of these crystal structure analyses failed, as the conformational changes and molecular shifts are relatively small and very complex in detail. No 'key' point in the structure could be identified, at which any stress or thermal motions could trigger the change in the molecular packing. *All* substituents move in some way in the phase transitions, and substantial movement of any substituent in one molecule must push away a certain part of a neighboring molecule. Therefore it appears that cooperative movements of *all* side groups are responsible for the thermosalient effect.

Comparison with NMR results

The details of a variable-temperature ^{13}C cross-polarization magic-angle spinning NMR study on polycrystalline (I) are described by Fattah, Twyman & Dobson (1992). The main results of this study are compared with those of the present investigation:

(i) In the NMR study, very similar spectra were observed for all three phases. This is consistent with our observation of very similar crystal structures.

(ii) In the NMR study of form II, two distinct carbonyl group resonances were observed, while the resonances of the two methyl groups could not be separated from each other. For form II the situation is reversed: two methyl, but only one carbonyl resonance are observed. This cannot be explained by the crystal structures, which show clearly that the two acetyl groups in the molecule are non-equivalent, and acetyl (3) in all three phases has significantly higher temperature factors than acetyl (4). This suggests that methyl and carbonyl resonances should be slightly separated in all three phases. In the phase transition, the conformational changes of the acetyl groups and also of their surroundings are small. Still, these changes must be substantial enough to cause the observed differences in the NMR signals.

(iii) The NMR data suggest the existence of significant dynamical fluctuations of at least two aromatic ring moieties in *all three* phases, but the resolution of the spectral lines is insufficient to identify the nature of these motions. Our crystallographic analyses show unusually high temperature factors for the ring atoms, but no alternative discrete sites. However, it has to be remembered that the crystallographic resolution is $\sim 1 \text{ \AA}$. There is only evidence for some disorder in one aromatic ring (5) in the low temperature phase.

(iv) The NMR data show no evidence for the existence of intermediate phases that might occur during the phase transitions.

Summary and discussion

(1) The title compound (Fig. 1) exhibits reversible phase changes that are accompanied by excessive mechanical agitation. Such *jumping* in phase transitions has earlier been observed in other compounds, but (to our knowledge) the structural origin for this phenomenon was never really understood.

(2) At room temperature, the title compound exists in two crystalline polymorphs and a glass form. Crystallization from ethanolic solution always yields needle-shaped crystals of the same polymorph (form II); the other crystal form (form I) is obtained by cooling below a phase transition at 11°C . A third polymorph (form III), which is not stable at room temperature, is obtained when crystals of form II are heated above a second phase transition at 70°C . The latter is accompanied by the mechanical jumps mentioned above. If heated further, the crystals melt; when cooled, the melt solidifies as a glass.

(3) The (reversible) phase transition form II ↔ form III is associated with changes of the macroscopic crystal morphology: as the transition takes place, a defined transition front quickly runs along the needle axis, which is accompanied by a kink of several degrees, and the needle length is changed by over 10% (the length reduces in the heating and increases in the cooling transitions). These abrupt changes of the crystal morphology certainly cause 'hopping' if the specimen is not fixed.

(4) Under the polarizing microscope, the crystals always have a pronounced fibrous appearance. X-ray reflections are rather diffuse, indicating an unusually large mosaic spread. These deficiencies increase when phase transitions are traversed. As a consequence, only X-ray data sets of limited quality could be collected particularly for crystals of forms I and III, which were obtained by passing form II through phase transitions. In refinement, only crystallographic R values around 0.09 are reached.

(5) Forms II and III have space group $P2_1/c$ (one molecule per asymmetric crystal unit) with signifi-

cantly different unit-cell constants. Form I, space group $P2_1/n$, has two molecules per asymmetric crystal unit (Table 1). The temperature dependence of the unit-cell constants was determined for forms II and III; the thermal expansion upon heating is anisotropic (Fig. 2). At the phase transition, the volume per molecule increases by $\sim 17 \text{ \AA}^3$ ($\Delta V/V \approx 2.0\%$).

(6) Surprisingly, the crystal structures of the three polymorphs are very similar. Despite the different space group and unit-cell content of forms I and II, and the large differences of unit-cell constants between forms II and III, the general arrangement and the orientation of the molecules is the same in all three crystal forms. The phase transitions are only accompanied by relatively small shifts of the molecules with respect to each other, and by conformational changes of the flexible side groups. In the transition I \rightarrow II, the slightly different conformation of the two symmetry-independent molecules of form I converges to the conformation of the single molecule per asymmetric crystal unit of form II.

(7) The title compound contains six flexible side groups, which *all* change their conformation to some degree in the phase transitions. In particular, the benzyl side chains may rotate around three covalent bonds, and exhibit considerable flexibility: in the phase transitions, the torsion angles flip up to over 70° (Table 4 and Fig. 6). Despite this flexibility, however, the overall conformation of the molecule always remains similar.

(8) The displacement parameters are unusually high in all crystal structures; this may be as a result of the large mosaic spread of the crystals. The benzyl side chains exhibit the largest thermal parameters, suggesting extensive thermal vibrations (Table 3 and Figs. 4, 5). This is consistent with the solid-state NMR study which showed high mobility of at least two benzyl groups in the crystal.

(9) The acetyl groups of the compound form a layer of $\text{C}-\text{H}\cdots\text{O}=\text{C}$ hydrogen bonds. The pattern of these interactions does not change in the phase transitions, but in the transition I \leftrightarrow II the internal symmetry alters as a result of the change in space group.

(10) Despite all efforts, the reason for the phase transitions and the jumping effect could not be elucidated from the crystal structures. The system was found to be very complex: the molecule under study has six flexible side groups (some of which show

extensive thermal vibrations or even disorder) that all undergo some cooperative conformational changes in the transitions, and it is not obvious why the re-arrangement has such drastic effects.

(11) One can argue whether the effect of jumping crystals is a 'fascinating phenomenon' (a term used by one referee of this study), or just 'not much more than a physical-mechanical curiosity' (as stated by the other referee). Either way, the effect remains unexplained from the present study. If the mechanism of any jumping crystals is to be explored in detail, it may be advisable to study crystals formed by simpler molecules.

This study was supported by the Bundesministerium für Forschung und Technologie, FKZ 03 SA1 FUB 6.

References

- ALLEN, F. H. (1986). *Acta Cryst.* **B42**, 515–522.
 D'ANS, J. & LAX, A. (1967). *Taschenbuch für Chemiker und Physiker*, 3rd ed., Vol. 1. Berlin: Springer Verlag.
 DESIRAJU, G. R. (1991). *Acc. Chem. Res.* **24**, 290–296.
 DING, J., HERBST, R., PRAEFCKE, K., KOHNE, B. & SAENGER, R. (1991). *Acta Cryst.* **B47**, 739–742.
 ETTER, M. C., MACDONALD, J. C. & BERNSTEIN, J. (1990). *Acta Cryst.* **B46**, 256–262.
 ETTER, M. C. & SIEDLE, A. R. (1983). *J. Am. Chem. Soc.* **105**, 641–643.
 FATTAH, J., TWYMAN, J. M. & DOBSON, C. M. (1992). *Magn. Reson. Chem.* **30**, 606–615.
 GIGG, J., GIGG, R., PAYNE, S. & CONANT, R. (1987). *J. Chem. Soc. Perkin Trans. 1*, pp. 2411–2414.
 JEITSCHKO, W. (1975). *Acta Cryst.* **B31**, 1187–1190.
 JEITSCHKO, W. (1988). Private communication.
 JOHNSON, C. K. (1976). *ORTEP*. Report ORNL-5138. Oak Ridge National Laboratory, Tennessee, USA.
 KOHNE, B., PRAEFCKE, K. & MANN, G. (1988). *Chimia*, **42**, 139–141.
 KULESHOVA, L. N. & ZORKY, P. M. (1980). *Acta Cryst.* **B36**, 2113–2115.
 NORTH, A. C. T., PHILLIPS, D. C. & MATTHEWS, F. S. (1968). *Acta Cryst.* **A24**, 351–359.
 SHELDRIK, G. M. (1976). *SHELX76*. Program for crystal structure determination. Univ. of Cambridge, England.
 SHELDRIK, G. M. (1985). *Crystallographic Computing*, edited by G. M. SHELDRIK, C. KRÜGER & R. GODDARD, pp. 175–189. Oxford Univ. Press.
 STEINER, TH., HINRICHS, W., GIGG, R. & SAENGER, W. (1988). *Z. Kristallogr.* **182**, 252–253.
 STEINER, TH. & SAENGER, W. (1992). *J. Am. Chem. Soc.* **114**, 10146–10154.
 SUTOR, D. J. (1963). *J. Chem. Soc.* pp. 1105–1110.
 TAYLOR, R. & KENNARD, O. (1982). *J. Am. Chem. Soc.* **104**, 5063–5070.